

Synthesis, Structure and Magnetic Property of a Cobalt(II) Metal-Organic Framework

Dong-Hui Chen,^[a,b] Tian-Lu Sheng,^[a] Xiao-Quan Zhu,^[a,b] Ling Lin,^[a,b] Yue-Hong Wen,^[a] Sheng-Min Hu,^[a] Rui-Biao Fu,^[a] and Xin-Tao Wu*^[a]

Abstract. The three-dimensional (3D) porous cobalt(II) metal-organic framework (MOF), $[\text{Co}_3(\text{L})_2(\text{DMA})_2(\text{MeOH})_2 \cdot 4(\text{DMA}) \cdot 6(\text{MeOH})]_n$ (**1**) [L = fully deprotonated 2,7-bis(4-benzoic acid)-*N*-(4-benzoic acid) carbazole, DMA = *N,N*-dimethylacetamide], was synthesized by hydrothermal reaction. Based on X-ray single-crystal diffraction, structural analysis indicates that complex **1** crystallizes in the monoclinic *C2/c* space group. Complex **1** possesses a 3,6-connected three-dimensional (3D) topological structure with a point symbol of

$\{4^2 \cdot 6\}_2 \{4^4 \cdot 6^2 \cdot 8^7 \cdot 10^2\}$ when a trinuclear Co^{II} cluster was regarded as 6-connected node and the organic ligands could be regarded as 3-connected linkers between the 6-connected nodes. The framework structure exhibits a one-dimension (1D) channel with an accessible void of 4223.0 \AA^3 , amounting to 42.8% of the total unit-cell volume (9862.0 \AA^3). Moreover, the magnetic properties of complex **1** were studied.

Introduction

Metal-organic frameworks (MOFs), assembled from organic ligands and metal nodes, have generated interests due to their potential applications in gas storage,^[1] separation,^[2,3] luminescence sensing,^[4,5] and catalysis.^[6] Compared with traditional organic and inorganic materials, MOFs show their flexibility in tunable structures, internal surface areas, and optical properties.^[7,8] However, the design strategies and synthesize methods of novel MOFs are still challenged. Selecting suitable ligands, which should have specific properties, is one of the key to synthesizing MOFs with desired properties.^[9]

Among the variety of organic ligands, carbazole-based ligands have attracted massive attention due to their eximious thermal and photochemical stability, outstanding optical-physical, and electrochemical properties.^[10,11] Carbazole could be functionalized at (2,7-), (3,6-) and N positions. In order to obtain novel carbazole-based MOFs, (2,7-) and N positions were functionalized and 2,7-bis(4-benzoic acid)-*N*-(4-benzoic acid) carbazole (H_3L) was synthesized.^[12–19] Compared to functionalized at 3,6 position, 2,7-carbazole-based ligands have better fluorescent property and lower bandgap.^[20] On the other hand, functionalized at N positions is beneficial to self-assembling of the porous MOFs.^[21]

Due to the properties of H_3L , a stable and rigid tricarboxylic acid ligand, its solvent thermal reaction with Co^{II} salts predicted to form a novel porous MOF. Herein, we report

the synthesis and structure of a three-dimensional (3D) metal-organic framework, $[\text{Co}_3(\text{L})_2(\text{DMA})_2(\text{MeOH})_2 \cdot 4(\text{DMA}) \cdot 6(\text{MeOH})]_n$ (**1**) [L = fully deprotonated 2,7-bis(4-benzoic acid)-*N*-(4-benzoic acid) carbazole, DMA = *N,N*-dimethylacetamide].

Results and Discussion

Crystal Structure of Complex 1

Singe-crystal X-ray diffraction study reveals that complex **1** crystallizes in the monoclinic *C2/c* space group. Structure analysis shows that complex **1** is a three-dimensional (3D) framework. The asymmetric unit possesses two fully deprotonated L ligands molecules, a linear trinuclear Co^{II} cluster, two coordinated DMA molecules, two coordinated methanol molecule, and several free solvent molecules. As shown in Figure 1, the three Co^{II} ions in the trinuclear Co^{II} cluster are in different coordinated environment. $\text{Co}^{\text{II}}(1)$ is six-coordinate by six carboxyl oxygen atoms of six L ligands and it is in the middle of the linear trinuclear Co^{II} cluster. Both $\text{Co}^{\text{II}}(2)$ and $\text{Co}^{\text{II}}(2')$ are five-coordinate by three carboxyl oxygen atoms of three L ligands, an oxygen atom from a DMA molecule, and an oxygen atom from a methanol molecule. Meanwhile, deprotonated L ligands molecules coordinate with trinuclear Co^{II} clusters as linkers and the 3D framework of complex **1** is obtained (Figure 2).

The $\text{Co}^{\text{II}}(1)$ –O bond lengths are in the range from 1.994(3) Å to 2.176(3) Å. The distances of $\text{Co}^{\text{II}}(2)/\text{Co}^{\text{II}}(2')$ –O range from 2.040(2) to 2.186(2) Å. The O– $\text{Co}^{\text{II}}(1)$ –O angles are varying from 83.18(14) to 173.30(14)° and the O– $\text{Co}^{\text{II}}(2)/\text{Co}^{\text{II}}(2')$ –O angles are ranging from 88.43(10) to 180.00(14)°. The selected bond lengths and bond angles for complex **1** are listed in Table S2 and Table S3 (Supporting Information).

Complex **1** is a 3D framework with a 1D channel, which has a diameter of 7.0 Å (Figure 3). A PLATON calculation

* Prof. X.-T. Wu
E-Mail: wxt@fjirsm.ac.cn

[a] State Key Laboratory of Structure Chemistry
Fujian Institute of Research on the Structure of Matter
Chinese Academy of Sciences
Fuzhou 350002, Fujian, P. R. China

[b] University of the Chinese Academy of Sciences,
Beijing, 100049, P. R. China

Supporting information for this article is available on the WWW under <http://dx.doi.org/10.1002/zaac.201700128> or from the author.

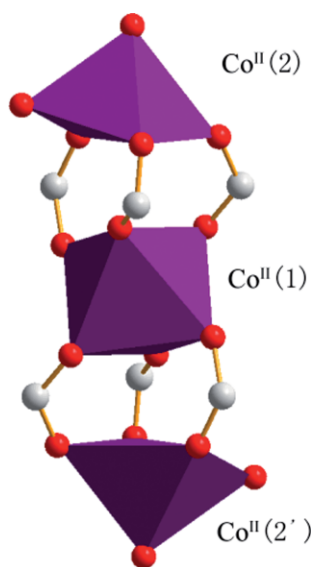


Figure 1. Secondary building units (SBUs) of complex **1**.

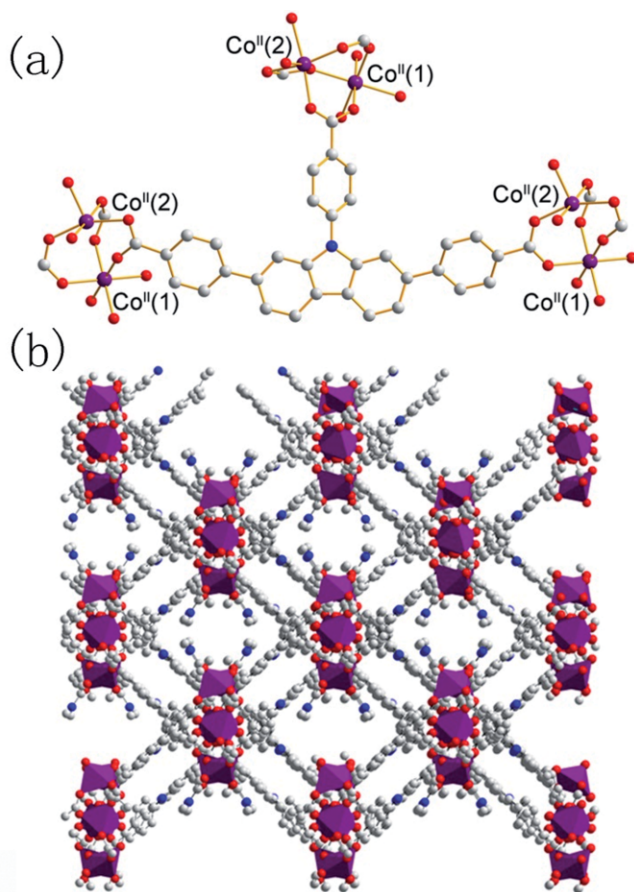


Figure 2. (a) Coordination environment of the deprotonated L ligand molecule. (b) Organic ligands connected by SBUs in complex **1**.

indicated that the total potential solvent volume when the free solvent molecules are removed is 4223.0 \AA^3 , which corresponds to 42.80% per unit cell volume (9862.0 \AA^3).

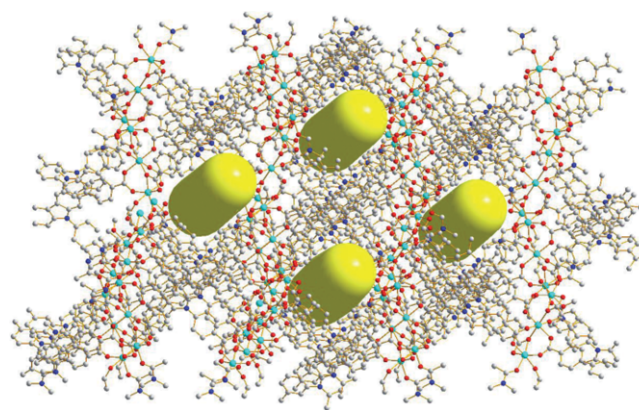


Figure 3. View of 1D channel in complex **1** indicated by a yellow cylinder.

Topologically, the metal node can be regarded as a 6-connected node and organic ligands can be regarded as a 3-connected linker between the metal nodes. The structure of complex **1** can be described as a 3,6-connected network with a Schläfli symbol of $\{4^2 \cdot 6\}_2\{4^4 \cdot 6^2 \cdot 8^7 \cdot 10^2\}$ (Figure 4).^[22]

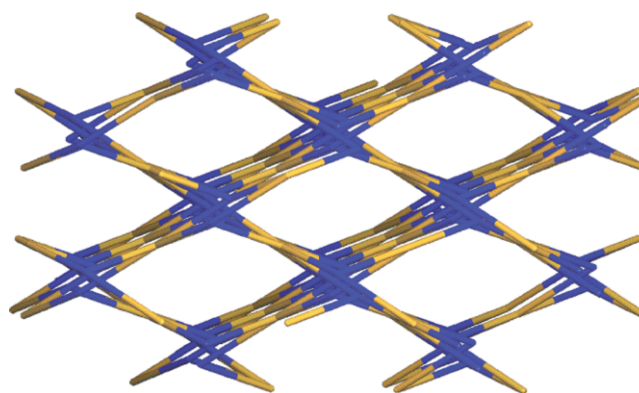


Figure 4. Topological representation of the 3,6-connected network in complex **1**.

X-ray Powder Diffraction

Powder X-ray diffraction (PXRD) for finely ground powder samples of complex **1** were carried out at room temperature. The experimental PXRD pattern corresponds well with the simulated pattern from the data of single-crystal X-ray diffraction, as shown in Figure 5.

Thermal Analysis

In order to estimate the thermal stability of complex **1**, thermogravimetric analysis (TGA) experiments were carried out on using polycrystalline samples of complex **1** (Figure 6). The TGA experiments were performed in a nitrogen atmosphere with a heating rate of $15 \text{ K} \cdot \text{min}^{-1}$ in the range of 30–900 °C. For complex **1**, a weight loss of 8% from room temperature to 100 °C is ascribed to the loss of free solvent molecules between the crystals. From 100 to 170 °C, free solvent molecules

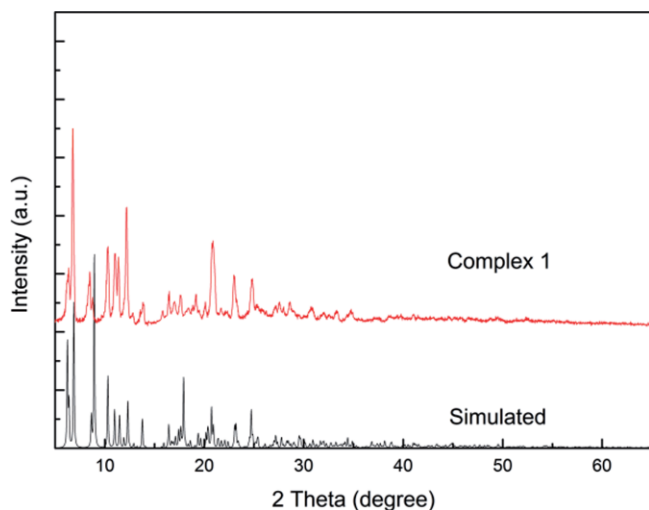


Figure 5. Simulated (black), experimental (red) powder X-ray diffraction (PXRD) patterns for complex **1**.

in the 1D channel of the framework were removed generally with a weight loss of 25%. After that, coordinated DMA and methanol molecules were detached gradually from 175 to 450 °C with a weight loss of 8%. The framework collapses and decomposes after 450 °C.

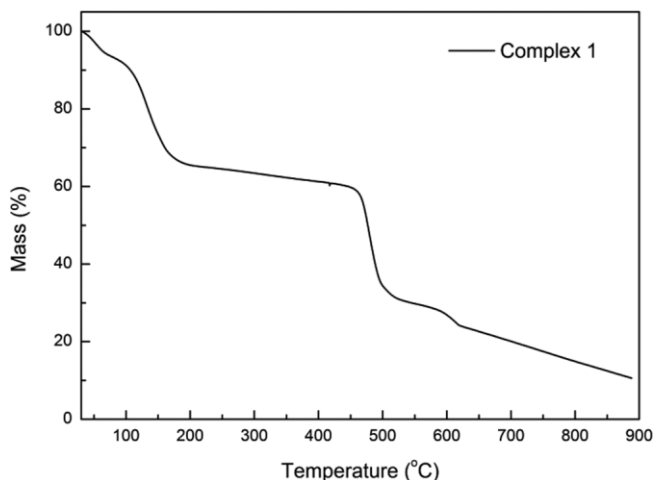


Figure 6. Thermal analysis curves of complex **1**.

Magnetic Properties

The magnetic properties were measured using a crystalline sample, whose phase purity was confirmed by powder X-ray diffraction. The temperature-dependent magnetic susceptibility of complex **1** was investigated in the range of 2–300 K at a direct current field of 1.0 kOe. As shown in Figure 7, the $\chi_{\text{m}}T$ value of complex **1** at 300 K is $8.19 \text{ cm}^3 \cdot \text{K} \cdot \text{mol}^{-1}$, which is appreciably higher than the expected value ($6.81 \text{ cm}^3 \cdot \text{K} \cdot \text{mol}^{-1}$) of three isolated spin-only Co^{II} ions ($S = 3/2$, $g = 2.20$).^[23–25] As shown in Figure 7, the χ_{M} of complex **1** obeys the Curie-Weiss law over the whole temperature range. In the temperature range of 2–300 K, the fit of the curve for

χ_{M}^{-1} vs. T plot to the Curie-Weiss law results in $C = 8.34 \text{ cm}^3 \cdot \text{K} \cdot \text{mol}^{-1}$ and $\theta = -4.38 \text{ K}$. The $\chi_{\text{M}}T$ value of complex **1** keeps steadily from room temperature to 150 K with decreasing temperature. This magnetic behavior is usually the signature of a paramagnetic effect of Co^{II} metal ions in the frameworks. Upon cooling, the $\chi_{\text{M}}T$ value of compound **1** rapidly decreased to a value of $6.49 \text{ cm}^3 \cdot \text{K} \cdot \text{mol}^{-1}$ at 7.5 K which may be due to the spin-orbit coupling and/or antiferromagnetic coupling between the three Co^{II} ions. The nearest distances of $\text{Co}^{2+} \cdots \text{Co}^{2+}$ in complex **1** is 3.52 \AA . Below 7.5 K, the $\chi_{\text{M}}T$ value of complex **1** increased abruptly to reach $6.80 \text{ cm}^3 \cdot \text{K} \cdot \text{mol}^{-1}$ at 2.5 K, and then decreased to $6.70 \text{ cm}^3 \cdot \text{K} \cdot \text{mol}^{-1}$ at 2.0 K, which may exhibit weak ferromagnetic behavior at low temperature between trinuclear Co^{II} clusters.^[26–32] The nearest distances between the trinuclear Co^{II} clusters in complex **1** is 10.15 \AA . The slight irregular vibration of $\chi_{\text{M}}T$ value may be attributed to interference of system noise and/or a small amount of impure substance.

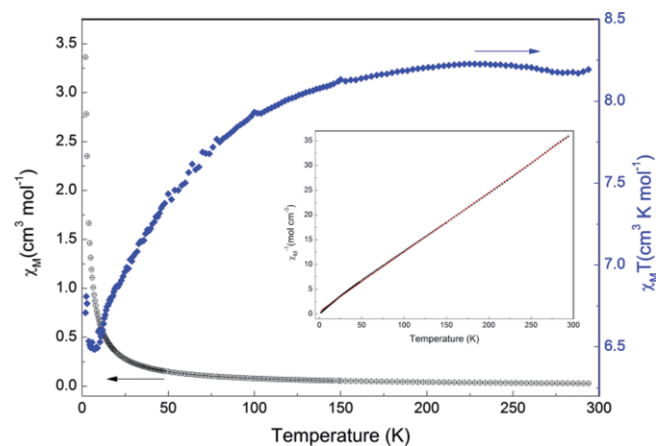


Figure 7. Thermal variation of χ_{M} and $\chi_{\text{M}}T$ for complex **1**. Insert: plot of the thermal variation of χ_{M}^{-1} for complex **1**.

N_2 Adsorption Properties

The N_2 adsorption property of complex **1** was measured at 77 K. As shown in Figure S2 (Supporting Information), the reversible N_2 sorption isotherm of complex **1** reveals a type-I N_2 adsorption ($25.14 \text{ cm}^3 \cdot \text{g}^{-1}$ at 1 atm) with a Brunnauer-Emmett-Teller (BET) surface area of $51.85 \text{ m}^2 \cdot \text{g}^{-1}$. We presume that the low N_2 adsorption may be due to the instability of the framework during the pretreatment of the BET measurement in vacuo, which is for removing the solvent molecules (DMA and MeOH) in the framework.

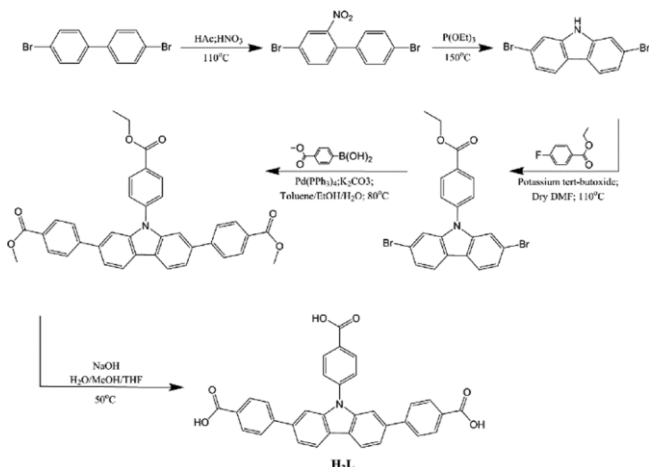
Conclusions

A porous metal-organic framework based on 2,7-bis(4-benzoic acid)-*N*-(4-benzoic acid) carbazole was synthesized and characterized. Complex **1** exhibits a 3,6-connected 3D framework with an 1D channel. The solvent-accessible volume is 42.8% of the total unit-cell volume as calculated by PLATON software. Magnetic measures show that complex **1** exhibits an

interesting magnetic transformation property. This MOF can possibly be utilized as novel porous material.

Experimental Section

Materials and Methods: Ethyl 4-fluorobenzoate, 4,4'-dibromobiphenyl, potassium *tert*-butoxide, potassium carbonate, $\text{Co}(\text{NO}_3)_2 \cdot 6\text{H}_2\text{O}$, tetrakis(triphenylphosphine)-palladium(0), and solvents were purchased commercially and used directly without further purification. As shown in Scheme 1, 2,7-bis(4-benzoic acid)-*N*-(4-benzoic acid) carbazole (H_3L) was synthesized following the reported procedure.^[19] Elemental analyses (C, H, N) were performed with an Elementar Vario EL-Cube Element Analyzer. Powder X-ray diffraction (PXRD) data were collected with a Rigaku MiniFlex 600 diffractometer using $\text{Cu-K}\alpha$ radiation ($\lambda = 0.154 \text{ nm}$). Thermogravimetric analysis (TGA) experiments were carried out with a NETZSCH STA 449C Jupiter thermogravimetric analyzer in flowing nitrogen with the sample heated in an Al_2O_3 crucible from room temperature to 1000°C at a heating rate of $10 \text{ K}\cdot\text{min}^{-1}$. Infrared spectra were recorded with KBr pellets in the range $4000\text{--}400 \text{ cm}^{-1}$ with a Perkin-Elmer Spectrum One FT-IR spectrometer. Magnetic susceptibilities of crystalline samples were measured with a Quantum Design MPMS-XL SQUID susceptometer under an applied magnetic field of 1 kOe in the $2\text{--}300 \text{ K}$ range. Diamagnetic corrections were made using Pascal's constants.^[33] The N_2 sorption isotherm of complex **1** was measured with a Micromeritics ASAP 2020 surface area and porosimetry analyzer at 77 K .



Scheme 1. Synthesis of 2,7-bis(4-benzoic acid)-*N*-(4-benzoic acid) carbazole (H_3L).

Synthesis of $[\text{Co}_3(\text{L})_2(\text{DMA})_2(\text{MeOH})_2 \cdot 4(\text{DMA}) \cdot 6(\text{MeOH})]_n$ (1**):** A solution of H_3L (0.026 g , 0.05 mmol) in DMA (1.5 mL) was directly mixed with a solution of $\text{Co}(\text{NO}_3)_2 \cdot 6\text{H}_2\text{O}$ (0.058 g , 0.2 mmol) in methanol (0.5 mL) at room temperature. The mixture was sealed in a 10 mL Teflon-lined autoclave and heated at 80°C for 96 h . After cooling to room temperature at a speed of $3 \text{ K}\cdot\text{h}^{-1}$, purple block crystals were collected (yield: 45% based on H_3L) (Figure 8). $\text{Co}_3\text{C}_{98}\text{H}_{122}\text{N}_8\text{O}_{26}$; calcd.: C 58.7 , H 6.13 N 5.58% ; found: C 58.8 , H 6.12 , N 5.58% . The UV/Vis spectrum of complex **1** is shown in Figure S1 (Supporting Information). **IR** (KBr): $\tilde{\nu} = 3594$ (w), 3067 (w), 3038 (w), 2926 (w), 1604 (vs), 1547 (s), 1510 (m), 1398 (vs), 1328 (m), 1255 (m), 1182 (m), 1142 (w), 1106 (w), 1015 (m), 947 (w), 853 (m), 819 (w), 783 (s), 740 (m), 709 (w), 653 (w), 597 (w), 562 (w), 484 (m) cm^{-1} .

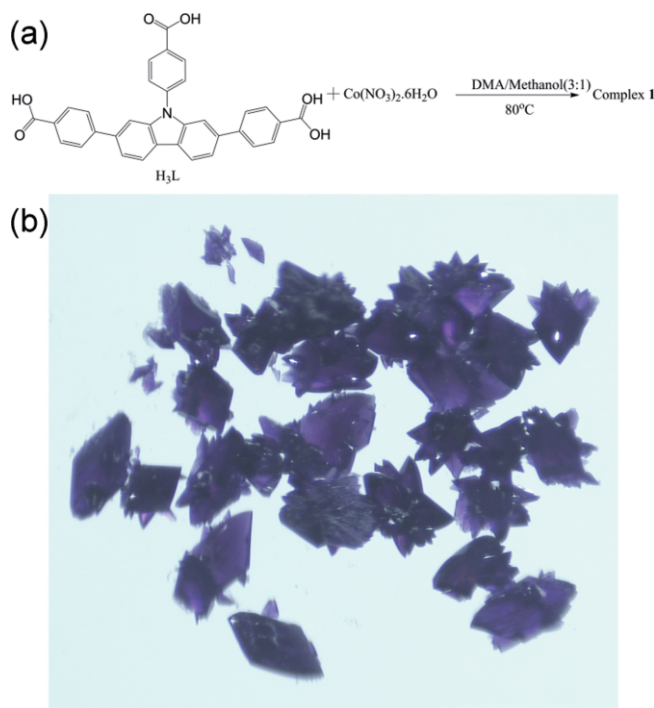


Figure 8. (a) Synthesis of complex **1**. (b) Crystals photo of complex **1**.

Crystal Structure Determination: A plum block crystal of complex **1** was selected carefully and glued on the top of a thin glass fiber for single-crystal X-ray diffraction data collection. The data were collected with a Rigaku Saturn 724HG CCD diffractometer (Mo $\text{K}\alpha$ radiation $\lambda = 0.71073 \text{ \AA}$ graphite-monochromator) at $293(2) \text{ K}$. The structure was solved by direct methods and refined by full-matrix least-squares of F^2 using the SHELX-97 program.^[34] Hydrogen atoms were added in their idealized positions and refined using a riding model. The SQUEEZE routine of the PLATON software suite was used in removing highly disordered solvent molecules. The final formulas were calculated according to the Squeeze results combined with the results from thermogravimetric analysis (TGA) and elemental analyses (EA).^[35,36] A total of 49968 reflections of complex **1** were collected in the range of $2.06 < \theta < 27.49^\circ$ ($-33 \leq h \leq 39$, $-21 \leq k \leq 21$, $-28 \leq l \leq 28$) and 11281 were independent with $R_{\text{int}} = 0.0415$. The final $R = 0.0668$ and $wR = 0.2071$ ($w = 1/[\sigma^2(F_o^2) + (0.1339P)^2 + 12.3872P]$, where $P = (F_o^2 + 2F_c^2)/3$). $S = 1.07$, $(\Delta/\sigma)_{\text{max}} < 0.001$, $\Delta\rho_{\text{max}} = 1.78 \text{ e}\cdot\text{\AA}^{-3}$, $\Delta\rho_{\text{min}} = -1.06 \text{ e}\cdot\text{\AA}^{-3}$. Crystal data and structure refinements are listed in Table 1. Selected bond lengths and bond angles for complex **1** are summarized in Table S1 and Table S2 (Supporting Information).

Crystallographic data (excluding structure factors) for the structure in this paper have been deposited with the Cambridge Crystallographic Data Centre, CCDC, 12 Union Road, Cambridge CB21EZ, UK. Copies of the data can be obtained free of charge on quoting the depositary number CCDC-1544683 (Fax: $+44\text{-}1223\text{-}336\text{-}033$; E-Mail: deposit@ccdc.cam.ac.uk, <http://www.ccdc.cam.ac.uk>).

Supporting Information (see footnote on the first page of this article): Additional selected bond lengths and angles, UV/Vis spectrum and N_2 isotherm volume.

Table 1. Crystal data and structure refinements for complex **1**.

	1
Empirical formula	C ₃ O ₃ C ₉₈ H ₁₂₂ N ₈ O ₂₆
Formula weight	2004.84
Crystal system	monoclinic
Space group	C2/c
<i>a</i> /Å	30.220(6)
<i>b</i> /Å	16.499(3)
<i>c</i> /Å	21.605(4)
<i>α</i> /°	90
<i>β</i> /°	113.720(2)
<i>γ</i> /°	90
<i>V</i> /Å ³	9863(3)
<i>Z</i>	4
Temperature /K	293(2)
<i>D</i> /Mg·m ⁻³	0.986
<i>μ</i> /mm ⁻¹	0.55
<i>F</i> (000)	3020
<i>R</i> ₁ ^a , <i>wR</i> ₂ ^b [<i>I</i> > 2σ(<i>I</i>)]	0.0668, 0.2071
<i>θ</i> ranges /°	2.06 to 27.51
<i>R</i> (int)	0.0415
<i>h k l</i> ranges	−33 ≤ <i>h</i> ≤ 39 −21 ≤ <i>k</i> ≤ 21 −28 ≤ <i>l</i> ≤ 28
GOF on <i>F</i> ²	1.072

a) $R = \sum \|F_o| - F_c| / \sum F_o$, b) $wR_2 = [\sum [w(F_o^2 - F_c^2)^2] / \sum [(F_o^2)^2]]^{1/2}$.

Acknowledgements

The authors gratefully acknowledge financial support from the National Natural Science Foundation of China (21233009 and 21203194), the 973 Program (2014CB845603), the Strategic Priority Research Program of the Chinese Academy of Sciences, Grant No. XDB20000000.

Keywords: 2,7-Bis(4-benzoic acid)-*N*-(4-benzoic acid) carbazole; Cobalt; Magnetic properties; Porous Co^{II} metal-organic framework

References

- L. D. Tran, J. Ma, A. G. Wong-Foy, A. J. Matzger, *Chem. Eur. J.* **2016**, *22*, 5509–5513.
- P. Q. Liao, X. W. Chen, S. Y. Liu, X. Y. Li, Y. T. Xu, M. Tang, Z. Rui, H. Ji, J. P. Zhang, X. M. Chen, *Chem. Sci.* **2016**, *7*, 6528–6533.
- J. B. DeCoste, G. W. Peterson, *Chem. Rev.* **2014**, *114*, 5695–5727.
- X. Sun, Y. Wang, Y. Lei, *Chem. Soc. Rev.* **2015**, *44*, 8019–8061.
- J. Zhao, Y. N. Wang, W. W. Dong, Y. P. Wu, D. S. Li, Q. C. Zhang, *Inorg. Chem.* **2016**, *55*, 3265–3271.
- H. Xu, X. F. Liu, C. S. Cao, B. Zhao, P. Cheng, L. N. He, *Adv. Sci.* **2016**, *3*, 1600048.
- J. L. Mendoza-Cortes, M. O’Keefe, O. M. Yaghi, *Chem. Soc. Rev.* **2009**, *38*, 1257–1283.
- Q. L. Zhu, Q. Xu, *Chem. Soc. Rev.* **2014**, *43*, 5468–5512.
- D. Liu, T. F. Liu, Y. P. Chen, L. Zou, D. Feng, K. Wang, Q. Zhang, S. Yuan, C. Zhong, H. C. Zhou, *J. Am. Chem. Soc.* **2015**, *137*, 7740–7746.
- I. T. Choi, M. J. Ju, S. H. Kang, M. S. Kang, B. S. You, J. Y. Hong, Y. K. Eom, S. H. Song, H. K. Kim, *J. Mater. Chem. A* **2013**, *1*, 9114–9121.
- A. D. Finke, D. E. Gross, A. Han, J. S. Moore, *J. Am. Chem. Soc.* **2011**, *133*, 14063–14070.
- J. R. Li, A. A. Yakovenko, W. Lu, D. J. Timmons, W. Zhuang, D. Yuan, H. C. Zhou, *J. Am. Chem. Soc.* **2010**, *132*, 17599–17610.
- Y. Ooyama, N. Yamaguchi, I. Imae, K. Komaguchi, J. Ohshita, Y. Harima, *Chem. Commun.* **2013**, *49*, 2548–2550.
- L. Li, S. Tang, X. Lv, M. Jiang, C. Wang, X. Zhao, *New J. Chem.* **2013**, *37*, 3662–3670.
- A. B. Kumar, J. M. Anderson, R. Manetsch, *Org. Biomol. Chem.* **2011**, *9*, 6284–6292.
- P. P. Bag, D. Wang, Z. Chen, R. Cao, *Chem. Commun.* **2016**, *52*, 3669–3672.
- H. J. Cheng, X. Y. Tang, R. X. Yuan, J. P. Lang, *CrystEngComm* **2016**, *18*, 4851–4862.
- J. Jia, X. Lin, C. Wilson, A. J. Blake, N. R. Champness, P. Hubberstey, G. Walker, E. J. Cussen, M. Schroder, *Chem. Commun.* **2007**, 840–842.
- D. H. Chen, L. Lin, T. Sheng, Y. Wen, S. Hu, R. Fu, C. Zhuo, H. Li, X. Wu, *CrystEngComm* **2017**, *19*, 2632–2643.
- X. Liu, Y. Sun, Y. Zhang, F. Miao, G. Wang, H. Zhao, X. Yu, H. Liu, W. Y. Wong, *Org. Biomol. Chem.* **2011**, *9*, 3615–3618.
- B. Hu, X. Lv, J. Sun, G. Bian, M. Ouyang, Z. Fu, P. Wang, C. Zhang, *Org. Electron.* **2013**, *14*, 1521–1530.
- V. A. Blatov, *Struct. Chem.* **2012**, *23*, 955–963.
- C. M. Liu, D. Q. Zhang, D. B. Zhu, *Chem. Commun.* **2016**, *52*, 4804–4807.
- M. C. Dul, E. Pardo, R. Lescouëzec, Y. Journaux, J. Ferrando-Soria, R. Ruiz-García, J. Cano, M. Julve, F. Lloret, D. Cangussu, C. L. M. Pereira, H. O. Stumpf, J. Pasán, C. Ruiz-Pérez, *Coord. Chem. Rev.* **2010**, *254*, 2281–2296.
- H. S. Lu, L. Bai, W. W. Xiong, P. Li, J. Ding, G. Zhang, T. Wu, Y. Zhao, J. M. Lee, Y. Yang, B. Geng, Q. Zhang, *Inorg. Chem.* **2014**, *53*, 8529–8537.
- H. X. Zhang, Q. X. Yao, X. H. Jin, Z. F. Ju, J. Zhang, *CrystEngComm* **2009**, *11*, 1807–1810.
- X. C. Wang, Y. Chen, H. Yuan, Q. Yang, X. S. Zeng, H. J. Qiu, D. R. Xiao, *Z. Anorg. Allg. Chem.* **2016**, *642*, 724–729.
- M. Cortijo, P. Delgado-Martínez, R. González-Prieto, S. Herrero, R. Jiménez-Aparicio, J. Perles, J. L. Priego, M. R. Torres, *Inorg. Chim. Acta* **2015**, *424*, 176–185.
- J. Zhao, Y. Wang, W. Dong, Y. Wu, D. Li, B. Liu, Q. Zhang, *Chem. Commun.* **2015**, *51*, 9479–9482.
- J. Gao, K. Ye, M. He, W. W. Xiong, W. Cao, Z. Y. Lee, Y. Wang, T. Wu, F. Huo, X. Liu, Q. Zhang, *J. Solid State Chem.* **2013**, *206*, 27–31.
- H. Wang, J. Guo, X. Xu, P. Yao, Y. Jiang, *Trans. Met. Chem.* **2017**, *42*, 293–299.
- A. Rodríguez-Diéguez, S. Pérez-Yáñez, L. Ruiz-Rubio, J. M. Seco, J. Cepeda, *CrystEngComm* **2017**, *19*, 2229.
- G. A. Bain, J. F. Berry, *J. Chem. Educ.* **2008**, *85*, 532–536.
- G. M. Sheldrick, *SHELXL-97*, Program for Refining Crystal Structure Refinement, University of Göttingen, Germany, **1997**.
- A. L. Spek, *PLATON*, A Multipurpose crystallographic Tool; Utrecht University: Utrecht, The Netherlands, **2001**.
- Y. Wang, C. Tan, Z. Sun, Z. Xue, Q. Zhu, C. Shen, Y. Wen, S. Hu, Y. Wang, T. Sheng, X. Wu, *Chem. Eur. J.* **2014**, *20*, 1341–1348.

Received: April 23, 2017

Published Online: July 17, 2017